

Cite this: *Chem. Commun.*, 2012, **48**, 9738–9740

www.rsc.org/chemcomm

Intracellular self-assembly of nanoparticles for enhancing cell uptake†

Qingqing Miao,^a Xiaoyu Bai,^a Yingying Shen,^b Bin Mei,^a Jinhao Gao,^c Li Li^b and Gaolin Liang^{*ac}

Received 9th July 2012, Accepted 17th August 2012

DOI: 10.1039/c2cc34899c

A radioactive probe (**1**) has been developed and applied to a condensation reaction and self-assembly of radioactive nanoparticles (*i.e.*, ¹²⁵I-NPs) intracellularly. Upon 160 min cellular efflux, the radioactivity retained in cells incubated with **1** was 4-fold more higher than that of those cells treated with a scrambled control probe (**1-Scr**).

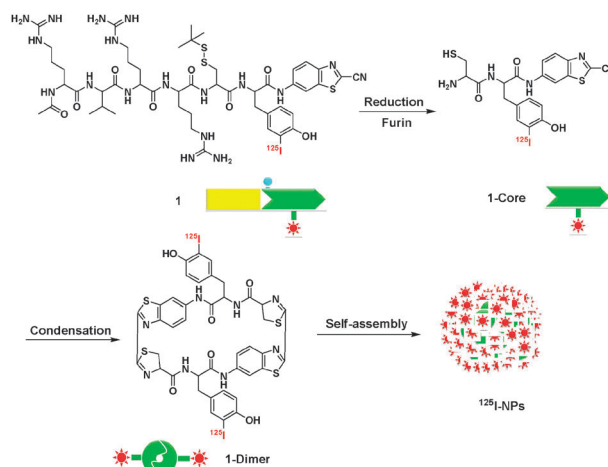
For cell imaging, most of the effort has been put on designing effective probes which can either easily overcome the cell membrane barriers or amplify their signals at the targeting site, or both.¹ For example, arginine-derived peptide for translocation through the negative charged phospholipid bilayer cell membrane,² ligand–receptor (folate–folate receptor, RGD–integrin $\alpha_v\beta_3$) interactions for effective cellular internalization.³ Avidin–biotin conjugations, or enzymatic reactions were applied on the probes to amplify their signals at the targeting sites.⁴ Some water-compatible “click” reactions also have been developed by chemists and applied for effective cellular labeling and imaging.⁵ In recent years, nanoprobe have emerged as an excellent tool for molecular imaging because of their ability of loading as many small molecular probes as needed to achieve the desired signal.⁶ Nevertheless, nanoprobe face the problems of cell membrane translocation and targeting, besides the difficulty and reproducibility of their fabrication.⁷

Self-assembly, a prevalent and important process in nature,⁸ provides an easy solution to the above problems. Up to date, a lot of self-assembly systems have been developed to make biocompatible nanomaterials for controlled drug release and delivery,⁹ biosensing,¹⁰ tissue engineering,¹¹ wound healing,¹² and even controlling the fate of cells.¹³ Nevertheless, using a lower concentration of small molecular probes to smartly self-assemble nanoprobe at the desired location in cells has still remained challenging and is less explored for molecular imagers.

Recently, Rao and co-workers developed a biocompatible condensation reaction between the 1,2-aminothiol group of cysteine and the cyano group of 2-cyanobenzothiazole (CBT) which could be controlled by pH, reduction and protease at concentrations as low as micromolar for self-assembly of nanostructures in living cells. This condensation reaction has shown promising applications for imaging protease activities in living cells, designing smart MRI probes, protein labeling, and so on.¹⁴

The trans-Golgi protease furin is a protein convertase that plays crucial roles in homeostasis, and in diseases ranging from anthrax and Ebola fever to Alzheimer’s disease and cancer.¹⁵ Overexpression of furin offers a useful hint of early development of certain cancers. One big advantage for chemists to study furin is that it preferentially cleaves Arg–X–Lys/Arg–Arg↓X motifs, where Arg is arginine, Lys is lysine, X can be any amino acid residue and ↓ indicates the cleavage site.¹⁶

Inspired by these, as shown in Scheme 1, we designed Acetyl–Arg–Val–Arg–Arg–Cys(StBu)–Tyr(I-125)–CBT (**1**) for self-assembling radioactive nanoparticles (¹²⁵I-NPs) under the action of furin in living tumor cells. After entering cells, the disulfide bond of the Cys motif of **1** is reduced by the intracellular glutathione (GSH) and subsequently its RVRRR motif is cleaved by furin on site, resulting in the active intermediate **1-Core**. Two **1-Cores** condense quickly to yield the amphiphilic dimer (*i.e.*, **1-Dimer**) which has a hydrophobic macrocyclic core



Scheme 1 Furin-controlled condensation of **1** to assemble radioactive nanoparticles in tumor cells.

^a CAS Key Laboratory of Soft Matter Chemistry, Department of Chemistry, University of Science and Technology of China, 96 Jinzhai Road, Hefei, Anhui, 230026, P. R. China. E-mail: gliang@ustc.edu.cn; Fax: +86-551-3600730; Tel: +86-551-3607935

^b State Key Laboratory of Oncology in Southern China, Imaging Diagnostic and Interventional Center, Cancer Center, Sun Yet-sen University, 651 Dongfeng Road East, Guangzhou, 510060, P. R. China

^c The Key Laboratory for Chemical Biology of Fujian Province, Xiamen University, Xiamen, 361005, P. R. China

† Electronic supplementary information (ESI) available: Experimental details and methods, synthesis of **1**, **1-Cold**, **1-Scr**, **1-Scr-Cold**, HPLC conditions, supplementary tables and figures (Scheme S1–S4, Table S1–S2, Fig. S1–S13). See DOI: 10.1039/c2cc34899c

for self-assembling ^{125}I -NPs via π - π stacking among each other. As-formed ^{125}I -NPs could concentrate the radioactivity inside cells on one hand. On the other hand, the big size and the hydrophobic property of the ^{125}I -NPs would prevent themselves from being pumped out by the cells. Compared with the control probes (e.g., scrambled control **1-Scr**) which could not be cleaved by furin or self-assemble in cells, **1** should have an enhanced cellular uptake by tumor cells, suggesting its promising application in tumor imaging *in vivo*.

We began the study with the synthesis and preparation of four compounds (two pairs): **1** and **1-Cold**, **1-Scr** and **1-Scr-Cold** (Fig. 1 and ESI†). To validate furin-controlled condensation and self-assembly, we used **1-Cold** for *in vitro* study. As shown in Fig. 2a, after 16 h incubation of **1-Cold** at 100 μM and 30 $^{\circ}\text{C}$ with 1 nmol U^{-1} of furin, we directly injected the incubation mixture into a HPLC system and collected the peaks for matrix-assisted laser desorption/ionization (MALDI) mass spectroscopic analysis. Peaks on HPLC traces at retention times of 44.2 min (41.8%), 47.3 min (3.0%) and 48.3 min (4.6%) were identified as the condensation products of **1-Cold** (i.e., **1-Cold-Dimer**, Fig. S1a and b, ESI†). The peak at retention time of 49.7 min (6.2%) was identified as the reduced product of **1-Cold** (i.e., **1-Cold-Red**, Fig. S1c, ESI†). Increasing the concentration of furin affords more condensation product **1-Cold-Dimer** within a shorter time. At 8 h and a furin concentration of 0.5 nmol U^{-1} , more of the **1-Cold** was cleaved and condensed to form **1-Cold-Dimer** which self-assembled into nanoparticles and changed the solution into a monodispersion. UV-Vis spectrum at 500–700 nm of the monodispersion showed an obvious increase of absorption compared with that of starting solution, suggesting the aggregation of nanoparticles (Fig. S2, ESI†). Dynamic light scattering (DLS) measurements indicated that the sizes of the nanoparticles have a narrow distribution and a mean diameter of 534 nm (Fig. 2b). Directly taking the above dispersion for transmission electron microscopy (TEM) observations, we found the nanoparticles have an average diameter of 388 nm (Fig. 2c). High magnification of the TEM images indicated that each nanoparticle is formed *via* the aggregation of smaller nanoparticles with a mean diameter around 13 nm (Fig. S3, ESI†). HPLC and MALDI mass spectroscopic analysis indicated that at least 77.3% of **1-Cold** was converted into its dimeric products

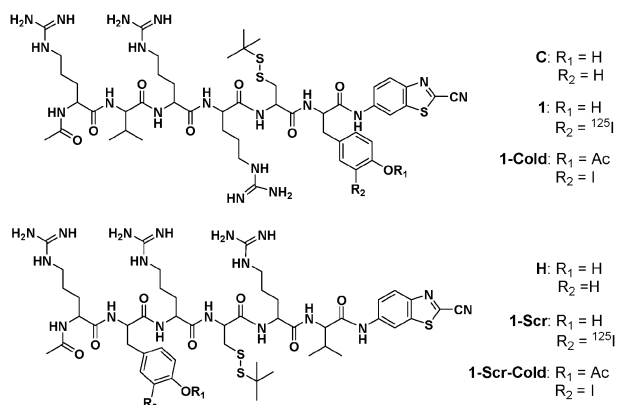


Fig. 1 Chemical structures of **C**, **1** and **1-Cold** for furin-controlled condensation and self-assembly, and their scrambled controls **H**, **1-Scr** and **1-Scr-Cold** respectively.

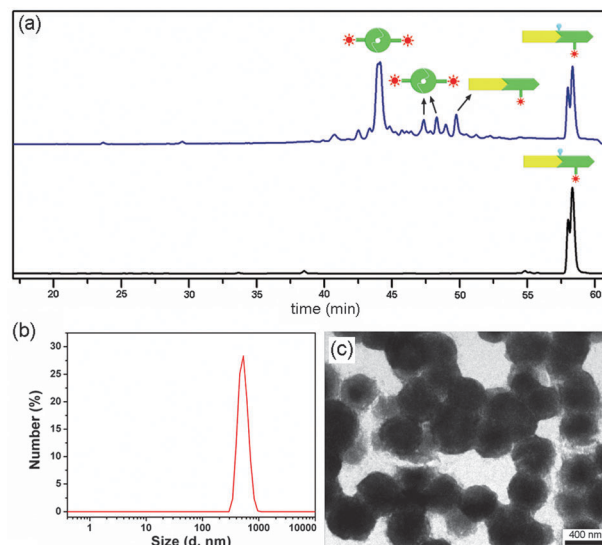


Fig. 2 (a) HPLC trace of the incubation mixture of **1-Cold** at 100 μM after 16 h incubation with 1 nmol U^{-1} of furin at 30 $^{\circ}\text{C}$ (upper), and HPLC trace of **1-Cold** in water (lower). (b) Dynamic light scattering (DLS) analysis of particles-size distribution of the self-assembled products of **1-Cold** after 8 h incubation with furin at 0.5 nmol U^{-1} and 30 $^{\circ}\text{C}$. (c) TEM images of the nanoparticles in b.

(i.e., **1-Cold-Dimer**) and only 6.3% of **1-Cold** was unacted (Fig. S4, ESI†).

After the validation of furin-controlled condensation and self-assembly, we started to use MDA-MB-468 cells to assemble ^{125}I -NPs intracellularly because we have demonstrated that MDA-MB-468 cells overexpress furin using furin immunofluorescence staining (Fig. S5, ESI†). Firstly, we studied the cell permeability of **1** and **1-Scr** by incubating the probes with MDA-MB-468 cells and quantitating the cellular uptake by counting the radioactivity with a γ -counter. Cellular uptake of both radiotracers rapidly reached their plateaus at 30 min (21.3% and 15.8% of total radioactivity for **1** and **1-Scr** respectively) during the 1 h experiments, with that of **1** being significantly higher than that of **1-Scr** at all time points (Fig. S6, ESI†). This result suggested that both **1** and **1-Scr** have excellent properties for cell permeability, and **1** is better than **1-Scr**, proven by the fluorescence microscopic images of the cells incubated with **1-Cold** or **1-Scr-Cold** respectively (Fig. S7, ESI†). After 8 h incubation with 100 μM of **1-Cold**, electron microscope (EM) image of the cells undoubtedly indicated that the locations of the intracellular nanoparticles were near/at Golgi bodies, the sites where furin is activated (Fig. S8, ESI†).

Although **1** might be directly applied for intracellular self-assembly of ^{125}I -NPs, there are still two potential problems which might hinder it from intracellular self-assembly. Firstly, even the radioactivity of **1** entering cells is high enough for detection, its chemical concentration might not high enough for initiating the condensation reaction for self-assembly. Secondly, intracellular free cysteine might react with the cyano group of **1** before it condenses with each other, resulting in the formation of **1-Dimer** and rendering its subsequent self-assembly infeasible.^{14c} To overcome these difficulties, we proceeded the studies with the experiments of concentration-dependent intracellular condensation. This was done by incubating 1 million

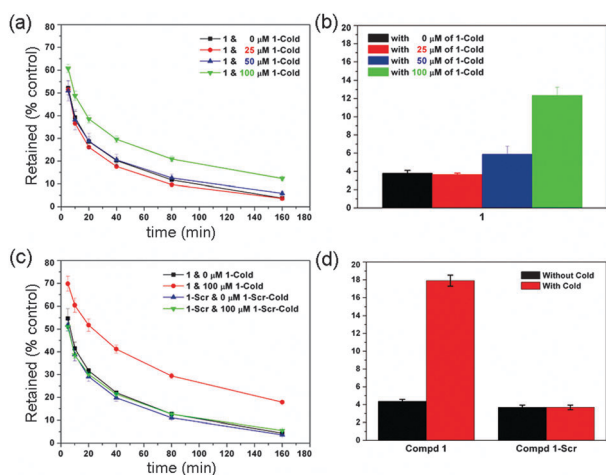


Fig. 3 (a, b) Concentration-dependent intracellular self-assembly: Time course of cellular efflux of **1** after 30 min incubation with 1 million MDA-MB-468 cells at 1 μ Ci and co-incubated with **1-Cold** at different concentrations (a). Radioactivity retained in cells after 160 minutes' efflux (b). (c, d) Effect of co-incubation on cellular efflux and retaining of radioactivity in MDA-MB-468 cells: Time course of cellular efflux of **1** and **1-Scr** after 30 min incubation with 1 million MDA-MB-468 cells with/without co-incubation of **1-Cold** or **1-Scr-Cold** at 100 μ M (c). Radioactivity retained in cells after 160 minutes' efflux (d). The dosage was normalized with that of 0 min (*i.e.*, after 30 minutes' incubation and before the efflux starts).

MDA-MB-468 cells with 1 μ Ci of **1** and different concentrations of **1-Cold**, we studied the cellular uptake and subsequent cellular efflux by counting the radioactivity retained inside the cells. As shown in Fig. 3a, co-incubation of 25 μ M or 50 μ M of **1-Cold** with **1** did not show obviously different cellular efflux curves compared with that of 0 μ M. However, cells co-incubated with 50 μ M of **1-Cold** showed significantly higher retaining of radioactivity than that of the control group after 160 min efflux (5.9% and 3.8% respectively, Fig. 3b), suggesting that 50 μ M of **1-Cold** is high enough for quenching the intracellular free cysteine and helping the condensation of **1**. Those cells incubated with 100 μ M of **1-Cold** and 1 μ Ci of **1** not only exhibited a different cellular efflux curve but also showed much more enhanced retention of radioactivity in cells at 160 min compared with that of the control group (12.3% and 3.8% respectively, Fig. 3a and b). After this, we studied the intracellular self-assembly of $^{125}\text{I-NPs}$ for enhancing cellular uptake. Four groups of MDA-MB-468 cells were studied in parallel (Group 1: 1 million cells incubated with 1 μ Ci of **1**, Group 2: with 1 μ Ci of **1** and 100 μ M of **1-Cold**, Group 3: with 1 μ Ci of **1-Scr**, and Group 4: with 1 μ Ci of **1-Scr** and 100 μ M of **1-Scr-Cold**). We used 100 μ M of **1-Cold** or **1-Scr-Cold** for co-incubation because we have proved that 100 μ M of **1-Cold** is suitable for furin cleavage and self-assembly of big nanoparticles (Fig. 2). As shown in Fig. 3c, only those cells in group 2 that were incubated with **1** and 100 μ M of **1-Cold** exhibited higher cell retention than those of the other three groups. After 160 min cellular efflux, radioactivity retained in MDA-MB-468 cells of

group 2 was 4-fold more higher than those of other three groups (4.4%, 17.9%, 3.7% and 3.7% for group 1–4 respectively, Fig. 3d), suggesting that intracellular $^{125}\text{I-NPs}$ actually help the retaining of radionuclide in living cells. Subsequent 3-(4,5-dimethylthiazol-2-yl) 2,5 diphenyl tetrazolium bromide (MTT) assay indicated that neither **1-Cold** nor **1-Scr-Cold** shows acute cytotoxicity to the cells at 100 μ M (Fig. S9, ESI†).

In summary, using a strategy of co-incubation, we have successfully demonstrated that intracellular condensation and subsequent self-assembly of nanoparticles could help the retaining of radionuclide in living tumor cells. This strategy starts with small molecules outside tumor cells but ends up with nanostructures inside them, offering a new method of designing “smart” probes for molecular imaging. Using this strategy for specifically imaging tumors *in vivo*, this research work is underway.

This work was supported by the National Natural Science Foundation of China (21175122, 91127036), the Fundamental Research Funds for Central Universities (WK2060190018), and Anhui Provincial Natural Science Foundation (1108085J17).

Notes and references

- M. F. Kircher, S. S. Gambhir and J. Grimm, *Nat. Rev. Clin. Oncol.*, 2011, **8**, 677.
- S. Futaki, I. Nakase, T. Suzuki, Y. J. Zhang and Y. Sugiura, *Biochemistry*, 2002, **41**, 7925.
- S. Santra, C. Kaitanis, O. J. Santiesteban and J. M. Perez, *J. Am. Chem. Soc.*, 2011, **133**, 16680.
- C. Y. Cao, Y. Chen, F. Z. Wu, Y. Deng and G. L. Liang, *Chem. Commun.*, 2011, **47**, 10320.
- (a) S. T. Laughlin, J. M. Baskin, S. L. Amacher and C. R. Bertozzi, *Science*, 2008, **320**, 664; (b) A. J. Link and D. A. Tirrell, *J. Am. Chem. Soc.*, 2003, **125**, 11164.
- (a) M. K. So, C. J. Xu, A. M. Loening, S. S. Gambhir and J. H. Rao, *Nat. Biotechnol.*, 2006, **24**, 339; (b) X. H. Gao, Y. Y. Cui, R. M. Levenson, L. W. K. Chung and S. M. Nie, *Nat. Biotechnol.*, 2004, **22**, 969.
- G. A. Silva, *Nat. Rev. Neurosci.*, 2006, **7**, 65.
- G. A. Silva, C. Czeisler, K. L. Niece, E. Beniash, D. A. Harrington, J. A. Kessler and S. I. Stupp, *Science*, 2004, **303**, 1352.
- G. L. Liang, Z. M. Yang, R. J. Zhang, L. H. Li, Y. J. Fan, Y. Kuang, Y. Gao, T. Wang, W. W. Lu and B. Xu, *Langmuir*, 2009, **25**, 8419.
- G. L. Liang, K. M. Xu, L. H. Li, L. Wang, Y. Kuang, Z. M. Yang and B. Xu, *Chem. Commun.*, 2007, 4096.
- V. Jayawarna, M. Ali, T. A. Jowitt, A. E. Miller, A. Saiani, J. E. Gough and R. V. Uljin, *Adv. Mater.*, 2006, **18**, 611.
- Z. M. Yang, G. L. Liang, M. L. Ma, A. S. Abbah, W. W. Lu and B. Xu, *Chem. Commun.*, 2007, 843.
- Z. Yang, G. Liang, Z. Guo and B. Xu, *Angew. Chem., Int. Ed.*, 2007, **46**, 8216.
- (a) H. J. Ren, F. Xiao, K. Zhan, Y. P. Kim, H. X. Xie, Z. Y. Xia and J. Rao, *Angew. Chem., Int. Ed.*, 2009, **48**, 9658; (b) G. L. Liang, H. J. Ren and J. H. Rao, *Nat. Chem.*, 2010, **2**, 54; (c) D. Ye, G. Liang, M. L. Ma and J. Rao, *Angew. Chem., Int. Ed.*, 2011, **50**, 2275; (d) G. Liang, J. Ronald, Y. Chen, D. Ye, P. Pandit, M. L. Ma, B. Rutt and J. Rao, *Angew. Chem., Int. Ed.*, 2011, **50**, 6283.
- G. Thomas, *Nat. Rev. Mol. Cell Biol.*, 2002, **3**, 753.
- M. Hosaka, M. Nagahama, W. S. Kim, T. Watanabe, K. Hatsuzawa, J. Ikemizu, K. Murakami and K. Nakayama, *J. Biol. Chem.*, 1991, **266**, 12127.